Acta Biomed 2018; Vol. 89, Supplement 1: 175-185 DOI: 10.23750/abm.v89i1-S.7021

Review

Radiofrequency ablation of osteoid osteoma

Massimo De Filippo[1], Umberto Russo[1], Vito Roberto Papapietro[1], Francesco Ceccarelli[2], Fancesco Pogliacomi[2], Enrico Vaienti[2], Claudia Piccolo[3], Raffaella Capasso[4], Assunta Sica[5], Fabrizio Cioce[5], Mattia Carbone[6], Federico Bruno[7], Carlo Masciocchi[7], Vittorio Miele[8]

[1] Department of Radiology, Parma Hospital, Parma, Italy; [2] Università degli Studi di Parma, Department of Surgical Sciences, Parma, Italy [3] Azienda Ospedaliera Careggi, Dipartimento di Radiologia d'emergenza, Università di Firenze; [4] Department of Health Sciences, University of Molise, Campobasso, Italy; [5] Department of Internal and Experimental Medicine, Università degli Studi della Campania Luigi Vanvitelli, Naples, Italy; [6] Department of Radiology, Salerno Hospital, Salerno, Italy; [7] Department of Biotechnology and Applied Clinical Science, University of L'Aquila, L'Aquila, Italy; [8] Department of Radiology, Careggi University Hospital, Florence, Italy

Summary. Osteoid osteoma is a benign bone neoplasm with a reported incidence of 2-3% among all bone primary tumors. Although it is a small and benign lesion, it is often cause of patient complaint and discomfort. It is generally characterized by a long lasting, unremitting pain that typically exacerbates at night, often leading to sleep deprivation and functional limitation of the skeletal segment involved, with a significant reduction of patient daily life activities and consequent worsening of the overall quality of life. Over decades, complete surgical resection has represented the only curative treatment for symptomatic patients. In the last years, new percutaneous ablation techniques, especially radiofrequency ablation, have been reported to be a safe and effective alternative to classical surgery, with a low complication and recurrence rate, and a significant reduction in hospitalization cost and duration. The aim of this article is to provide an overview about the radiofrequency thermal ablation procedure in the treatment of osteoid osteoma. (www.actabiomedica.it)

Key words: interventional radiology, osteoid osteoma, bone tumors, radiofrequency ablation

Osteoid osteoma (OO) is a benign bone tumor of undetermined etiology firstly described by Jaffe in 1935 (1-5). OO accounts for 2-3% of all bone primary tumors with an incidence of 10-12% among all benign skeletal neoplasms (6-10). It is more frequent in adolescents and young adults with 50% of patients being aged between 10 and 20 years and it predominates in male, with a reported male-to-female ratio of 4:1 (11-15). Clinical presentation can vary depending on the location of the lesion; patients generally complain of localized, deep and unremitting pain that increases in intensity over time, typically gets worse at night and rapidly improves after salicylates or other NSAIDs administration. Soft tissue swelling and skin erythema may be present in OO in subcutaneous location. Duration of pain can vary from weeks to years before definitive diagnosis, depending on how typical the clinical presentation is and how early the diagnostic suspect is posed.

Location

OO may occur anywhere in the axial or appendicular skeleton, but the majority of cases arises in the diaphysis or metaphysis of long bones in the lower limb (Fig. 1), with more than half involving either the femur or the tibia. Juxta-articular or intra-capsular location is generally associated with joint effusion and may clinically resemble an inflammatory arthropathy. Less commonly affected sites are the small bones of hand and feet. 10-20% of all OOs are located in the

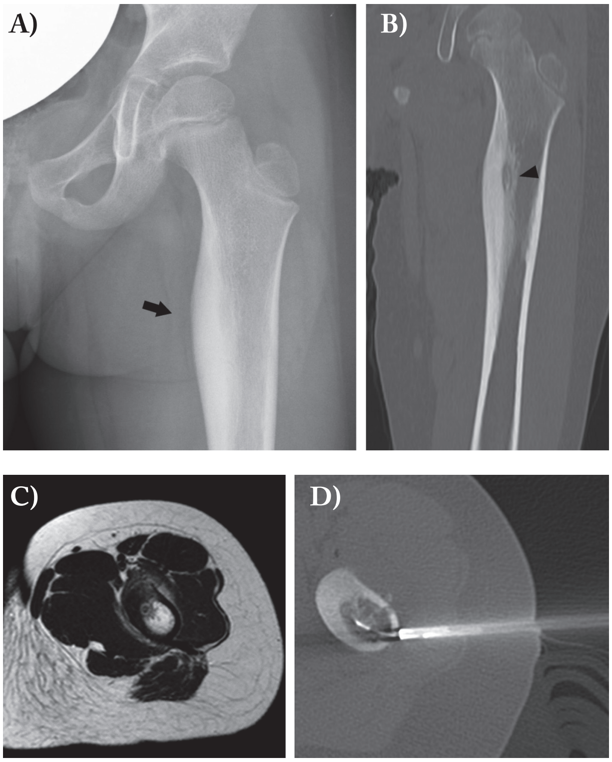

Figure 1. Osteoid osteoma of the proximal left femur. 6 year old female with left thigh pain of recent onset with no history of trauma. (A) Standard X-Ray shows wide cortical thickening of the medial portion of the proximal femoral diaphysis (arrow); radiolucent *nidus* is partially obscured by the surrounding reactive sclerotic bone. (B) MPR coronal view CT scan clearly demonstrates the presence of an oval shaped radiolucent *nidus* with some degree of calcification inside (arrowhead). (C) T2-weighted MRI image of the same lesion on the axial plane. (D) The lesion has been effectively treated with percutaneous radiofrequency thermal ablation

spine, with a predilection for the lumbar metamers; they almost exclusively occur in the posterior vertebral elements and they typically present with painful scoliosis (7, 11, 16-35).

Pathology

OO is structurally composed of a small central area of woven bone and osteoid matter, the *nidus*, surrounded by a zone of reactive sclerotic bone. The *nidus*, round or oval in shape, rarely exceeds 1,5-2 cm in diameter and may contain a central region of variable bone mineralization. According to its site of origin within the involved bone, OO can be classified in cortical, medullary (cancellous) and subperiosteal.

Cortical OO is the most common type and it generally presents with the classic central *nidus* and peripheral sclerosis as described above. Medullary OO is seen in the neck of the femur, in small bones and in the spinal column, while subperiosteal type is generally located on the intra-articular surface of the involved bone. Medullary and subperiosteal OO are less frequent and often demonstrate less peripheral bone sclerosis (Fig. 2), sometimes making their diagnosis more difficult (36-45).

Imaging

X-ray is the initial imaging modality in case OO is suspected. Plain radiograph typically shows a round or oval radiolucent *nidus*, usually smaller than 1,5 cm in diameter, surrounded by a variable but regular fusiform area of bone sclerosis (Fig. 1). In larger lesions, a central nucleus of bone mineralization within the *nidus* can also be observed. Sometimes the peripheral rim of reactive bone sclerosis is so extensive that the underlying radiolucent *nidus* may result obscured (46-61).

Computed Tomography is the imaging technique of choice for OO, being advantageous for detection and characterization of both the *nidus* and the peripheral sclerosis (Fig. 3). It is particularly helpful for small OOs, for those lesions which show less peripheral bone sclerosis (especially medullary and subperiosteal types), and in all those cases where standard radiographs are not clearly conclusive. On CT scan the *nidus* appears as a small well-defined radiolucent area, with soft-tissue attenuation values, which shows early vascular contrast enhancement (even if intravenous contrast administration is generally not necessary for definitive diagnosis). A variable degree of central *nidus* mineralization, sometimes punctate, is often seen (Fig. 4) (7, 46). Moreover, the presence of thin vascular grooves surrounding the lesion has been demonstrated to be highly specific for distinguishing OOs from other radiolucent bone tumors on CT (29, 62-70).

MRI is inferior to CT in diagnosing OO, although it is very sensitive in demonstrating bone marrow and perilesional soft tissues edema and inflammatory re-

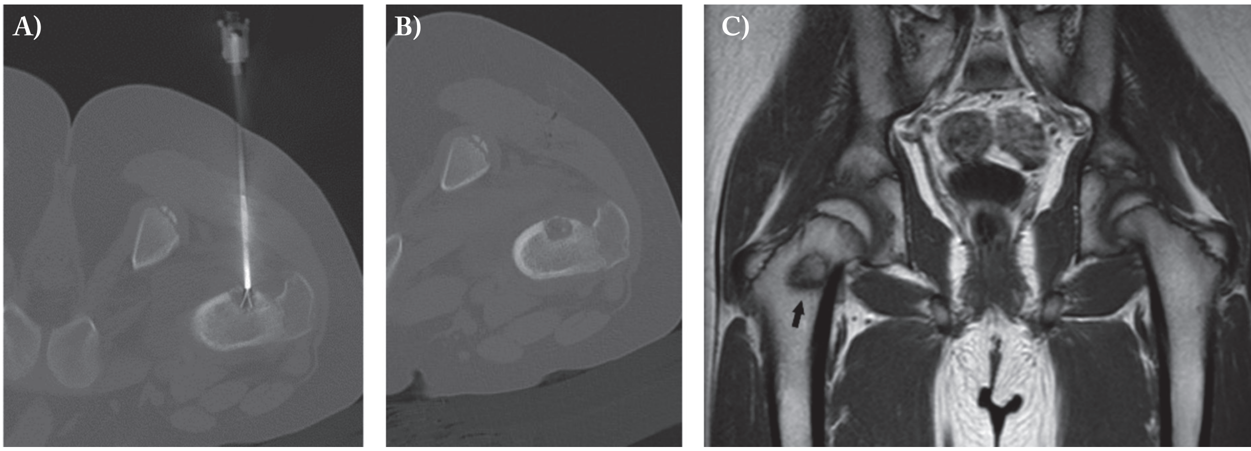

Figure 2. Osteoid osteoma of the right femoral neck. 12 year old male suffering from right hip pain irradiated to the omolateral thigh for several months was referred to our center for percutaneous treatment of an osteoid osteoma of the femoral neck; note that in this location osteoid osteoma generally shows less or absent peripheral sclerosis. (A) Radiofrequency ablation was achieved via a posterior trans-gluteal approach. (B) Post-procedural control CT scan. (C) 30 days post-treatment MRI showing regular outcomes of intervention (arrow)

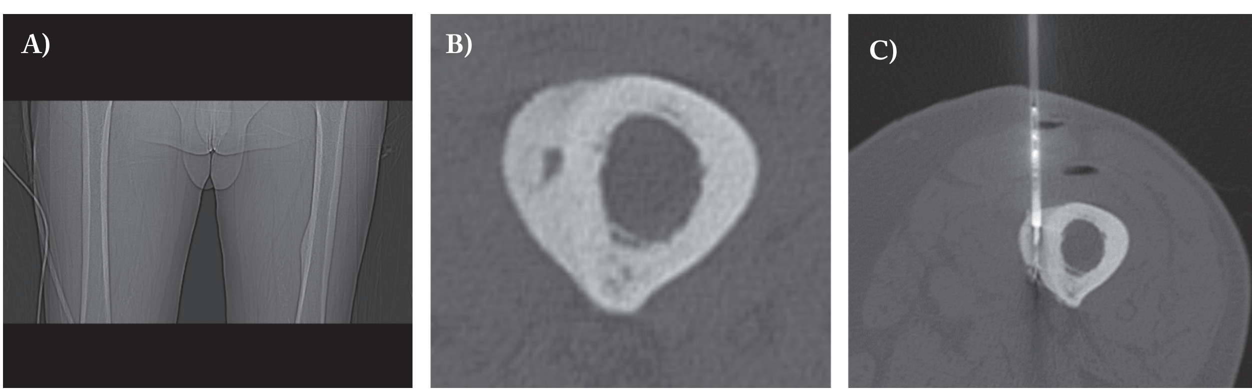

Figure 3. Osteoid osteoma of the femur in elderly patient. 71 year old male with unremittent left thigh pain; osteoid osteoma was not clinically suspected, since it is quite uncommon in this age range. (A) CT scanogram demonstrating the presence of focal cortical thickening of the left femoral diaphysis. (B) Classical CT appearance of osteoid osteoma: central radiolucent *nidus* surrounded by sclerotic reactive bone. (C) Radiofrequency ablation was effective in achieving complete resolution of the symptoms

action. The *nidus* generally shows low to intermediate signal intensity on T1-weighted images and variable intensity on T2-weighted images. Peripheral reactive sclerotic bone and central *nidus* calcifications are hypointense on both T1- and T2- weighted images (11, 36, 71-75). However, MRI findings should always be correlated to standard radiographs or CT since, when used alone, MRI can lead to a wrong diagnosis in a significant amount of cases (76-81).

Technetium-99-labeled bone scintigraphy typically reveals a central focus of intense radionuclide uptake (representing the *nidus*) surrounded by a larger region of less intense signal (corresponding to the reactive perilesional bone), the characteristic so-called “double-density” sign; it is seldom used today, due to concerns related to the isotope radioactivity (82-86).

Treatment

Although OOs can spontaneously regress in a period of time ranging from two to six years (87-

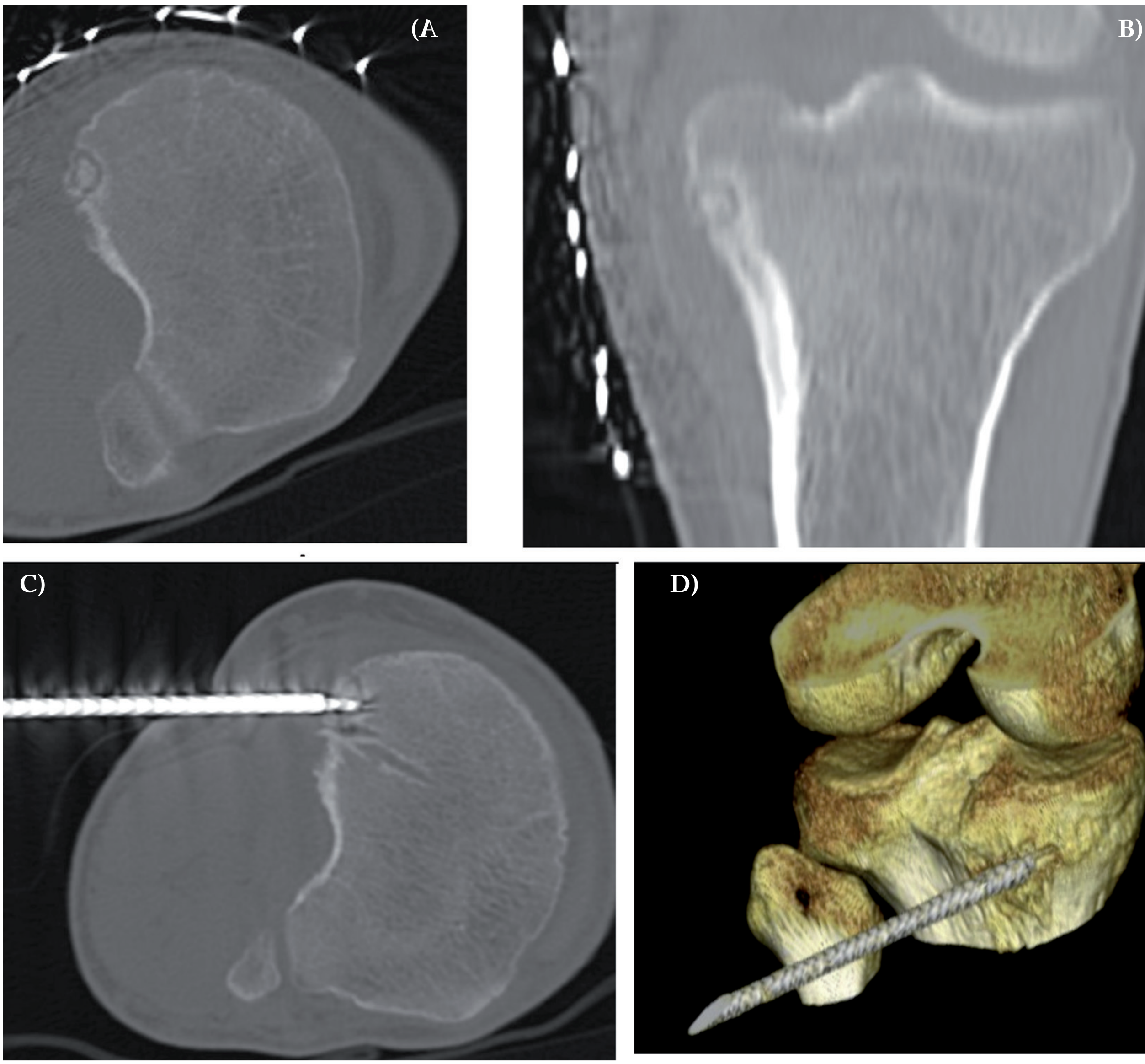

Figure 4. Osteoid Osteoma of the tibia. 20 year old male with long-standing left knee pain. (A, B) Axial and coronal plane images showing an osteoid osteoma near the posterior surface of the left tibia. (C) Percutaneous radiofrequency thermal ablation of the lesion. (D) Volume-rendering reconstruction of the positioning of the inserting cannula

90), over decades complete surgical excision has been considered the classical treatment for all those patients who had unremitting pain despite conservative treatment or those who could not tolerate long-term NSAIDs therapy. En bloc surgical resection has a reported success rate between 88% and 100% but it carries several significant disadvantages. Firstly, for the orthopedic surgeon it may be difficult to identify the precise location of the lesion and the exact amount of bone to resect; secondly, to be sure all the *nidus* is removed, a substantial volume of bone must be excised, potentially leading to bone weakness and consequent necessity of bone grafts, internal fixation and postoperative immobilization to prevent subsequent fractures. Nonetheless, recurrence rate remains significantly high (reported in literature to range from 4,5% to 25%) due to incomplete *nidus* excision (Fig. 5) (91-95).

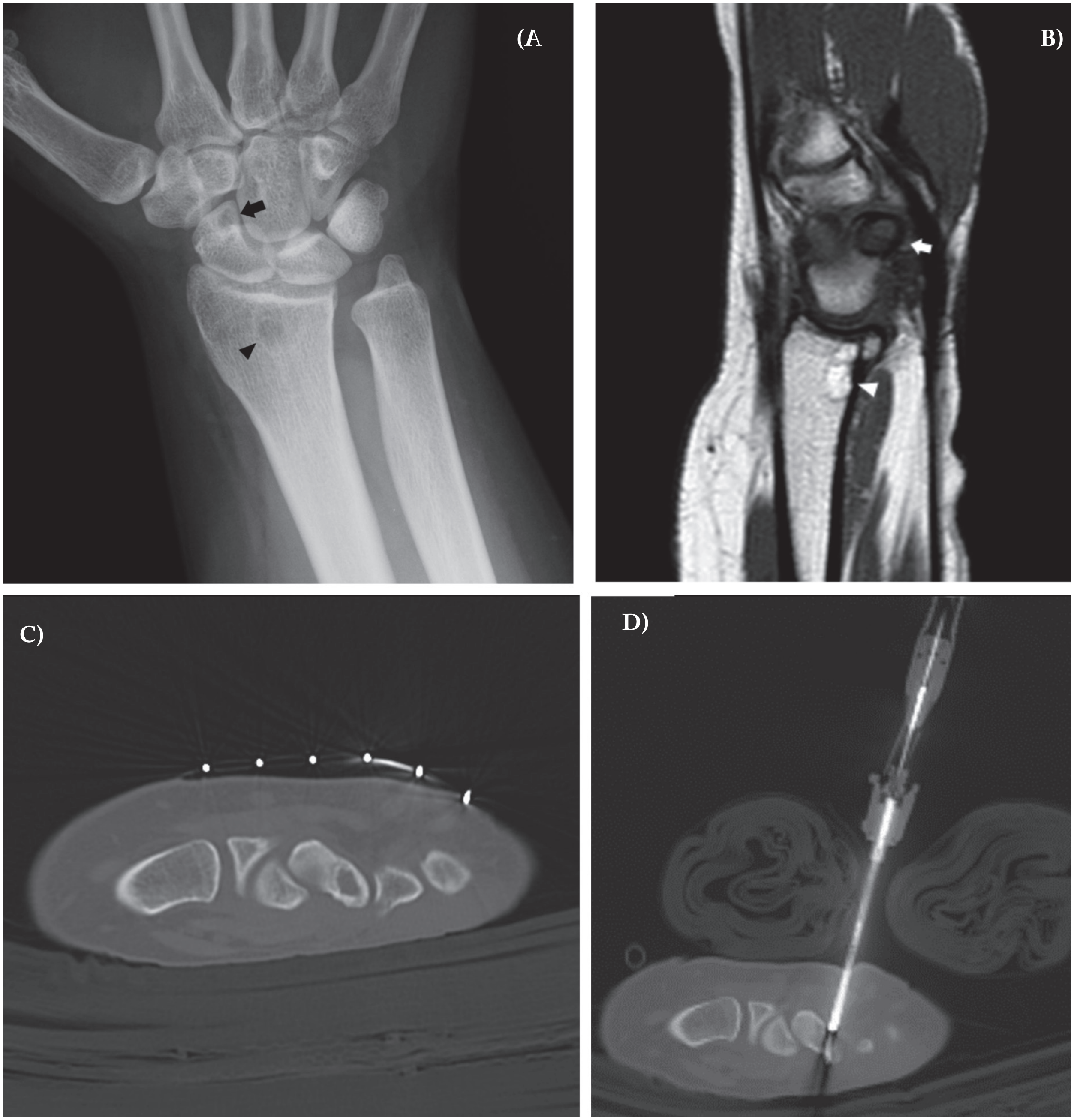

Fig. 5 Recurrence of osteoid osteoma after surgical curettage. 24 year old female complaining of persistent pain after surgical curettage of an osteoid osteoma of the scaphoid treated with bone graft from the distal radius. (A) Standard radiograph taken 3 months after the curettage shows the persistence of a radiolucent area at the distal pole of the right scaphoid (black arrow); missing bone from previous bone grafting (black arrowhead). (B) MRI confirmed the diagnosis of recurrence of osteoid osteoma (white arrow); note the outcomes of bone grafting from the distal radius (white arrowhead). (C-D) Radiofrequency ablation was the definitive treatment; wrist pain disappeared and no recurrence was observed.

Over the last years, percutaneous radiofrequency ablation (RFA) has been proposed as a new interventional technique for symptomatic patients with OO. It has widely and rapidly been accepted as a valid minimally invasive alternative to traditional orthopedic surgery, so much to be considered today the treatment of

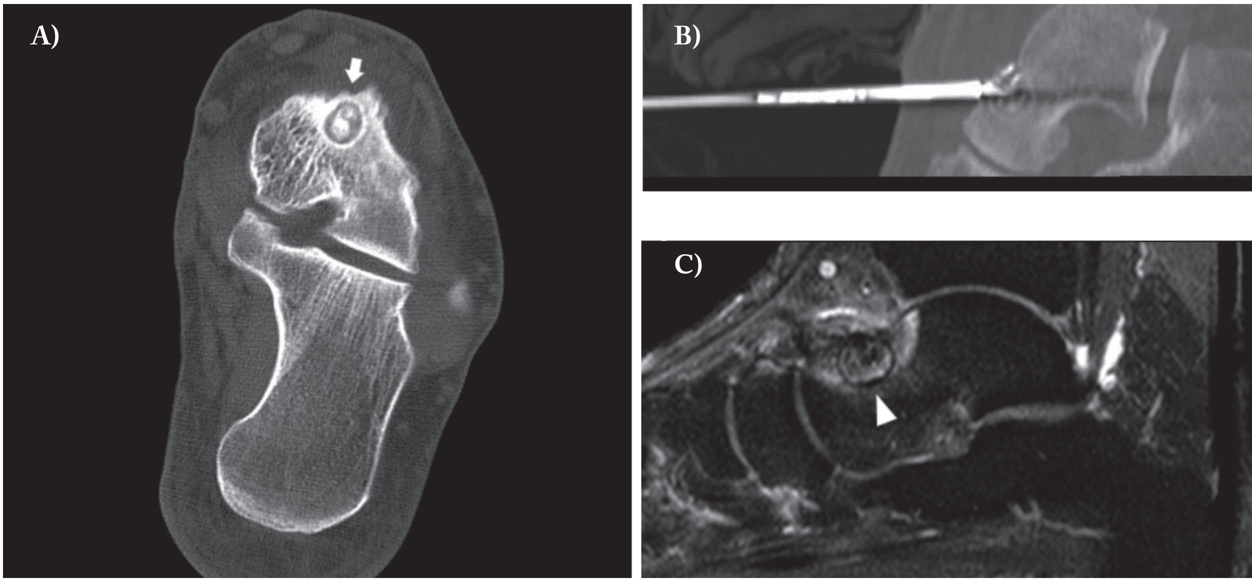

Figure 6. Osteoid osteoma of the talus. 39 year old male with recurrent left ankle pain. (A) CT scan demonstrates the presence of an osteoid osteoma of the talus (arrow). (B) Multiplanar reconstructions are used to guide the electrode inside the lesion. (C) 30 days post-treatment MRI showing regular thermal ablation outcomes (arrowhead)

choice for OOs, especially for those located in difficult areas for surgery (96-98). Percutaneous ablation is reported to be a safe and cost-effective treatment, with a superior long-term efficacy and a significant reduction in hospitalization cost and duration when compared to other surgical techniques. It has a reported success rate close to 100% and a recurrence rate of about 5% with almost negligible post-procedural complications (37, 99-106).

The procedure is performed in the CT room under aseptic conditions; patient position can be prone, supine or, more rarely, on lateral decubitus – depending on the location of the lesion. Two grounding pads are properly positioned on patient skin and connected to the RF generator. Local anesthesia is generally sufficient to control pain for all the duration of the operation, however the possibility to use general, spinal or epidural anesthesia is always discussed with the anesthesiologist (who is present in the CT room during the entire procedure), according to the patient collaboration and clinical conditions. CT scan is obtained to precisely localize the lesion and multi-planar reconstructions are used to plan the optimal trans-cutaneous approach. Close attention must be paid to adjacent blood vessels and nerves, since these structures must carefully be avoided. A penetration cannula with an inner stylet is introduced through the skin and soft tissue according to the previous established access route. New CT images are then obtained to verify the correct position of the cannula. Computed tomography has an extraordinary spatial resolution, but it carries the disadvantage that it cannot be used in real-time guidance; for this reason CT-fluoroscopy is increasingly adopted (107-113). Once ensured the distal end of the cannula is well positioned on the bone surface, the inner stylet is removed. Bone penetration is then accomplished by inserting – through the cannula – a Kirshner wire gradually tapped until the center of the *nidus*. Automatic orthopedic drill represents a feasible and helpful alternative for this step (114). Once within the *nidus*, the Kirshner wire is replaced with the ablation electrode (Fig. 6) and, after another accurate CT control of the electrode tip position, the electrode is connected to the RF generator. Whenever possible, once the *nidus* is accessible and before the electrode in inserted, a core biopsy of the lesion should be performed. When the electrode is documented to be exactly within the *nidus*, RFA starts. The lesion is generally heated to 90°C for a time of 5-6 minutes, which are widely reported to be the optimal ablation parameters. Lower temperatures would be ineffective or would significantly increase the ablation time. Higher temperatures can lead to tissue vaporization, a circumstance that would limit proper heat propagation through the lesion. Once the procedure is terminated, a last CT scan is obtained to exclude possible soft tissue damage. The electrode and the cannula are removed, local anesthetic is administered, and sterile dressing is applied to the skin entry site. The entire procedure can be performed in approximately 60 minutes. After a brief period of observation, all patients are generally discharged from hospital on the same day, with a 30 days scheduled follow-up visit and MRI control. Daily activities may immediately be resumed, with the exception for driving (101, 115-117). Post-procedural complications are rare, and may include skin burn, muscular hematoma, infection and nerve injury.

Conclusion

CT guided RFA is proven to be a safe and effective procedure for the treatment of OOs. When compared to surgical excision, it shows a significant reduction in hospitalization cost and duration. With its almost negligible post-procedural complications and a low rate of recurrence, RFA is at the moment the treatment of choice for these bone tumors.

References

1. Torg JS, Loughran T, Pavlov H, Schwamm H, Gregg J, Sherman M, Balduini FC. Osteoid osteoma. Distant, periarticular, and subarticular lesions as a cause of knee pain. Sports Med 1985; 2: 296-304.
2. Izzo R, Guarnieri G, Guglielmi G, Muto M. Biomechanics of the spine. Part I: Spinal stability. Eur J Radiol 2013; 82: 118-126.
3. Masala S, Nano G, Marcia S, Muto M, Fucci FPM, Simonetti G. Osteoporotic vertebral compression fracture augmentation by injectable partly resorbable ceramic bone substitute (Cerament™|SPINESUPPORT): A prospective nonrandomized study. Neuroradiology 2012; 54: 1245-1251.
4. Guarnieri G, Vassallo P, Pezzullo MG, Laghi F, Zeccolini F, Ambrosanio G, Galasso R, Muto M, Izzo R. A comparison of minimally invasive techniques in percutaneous treatment of lumbar herniated discs a review. Neuroradiol J 2009; 22: 108-121.
5. Cellerini M, Mangiafico S, Ammannati F, Ambrosanio G, Muto M, Galasso L, Mennonna P. Ruptured, dissecting posterior inferior cerebellar artery aneurysms: Endovascular treatment without parent vessel occlusion. Neuroradiology 2008; 50: 315-320.
6. Papathanassiou ZG, Megas P, Petsas T, Papachristou DJ, Nilas J, Siablis D. Osteoid osteoma: diagnosis and treatment. Orthopedics 2008; 31: 1118.
7. Iyer RS, Chapman T, Chew FS. Pediatric bone imaging: diagnostic imaging of osteoid osteoma. AJR Am J Roentgenol 2012; 198: 1039-52.
8. Lanzillo R, Prinster A, Scarano V, Liuzzi R, Coppola G, Florio C, Salvatore E, Schiavone V, Brunetti A, Muto M, Orefice G, Alfano B, Bonavita V, Brescia Morra V. Neuropsychological assessment, quantitative MRI and ApoE gene polymorphisms in a series of MS patients treated with IFN beta-1b. J Neurol Sci 2006; 245: 141-5.
9. Briganti F, Napoli M, Leone G, Marseglia M, Mariniello G, Caranci F, Tortora F, Maiuri F. Treatment of intracranial aneurysms by flow diverter devices: Long-term results from a single center. Eur J Radiol 2014; 83: 1683-1690.
10. Battipaglia G, Avilia S, Morelli E, Caranci F, Perna F, Camera A. Posterior reversible encephalopathy syndrome (PRES) during induction chemotherapy for acute myeloblastic leukemia (AML). Ann Hematol 2012; 91: 1327-1328.
11. Boscainos PJ, Cousins GR, Kulshreshtha R, Oliver TB, Papagelopoulos PJ. Osteoid osteoma. Orthopedics 2013; 36: 792-800.
12. Kransdorf MJ, Stull MA, Gilkey FW, Moser RP, Jr. Osteoid osteoma. Radiographics 1991; 11: 671-96.
13. Caranci F, Tedeschi E, Leone G, Reginelli A, Gatta G, Pinto A, Squillaci E, Briganti F, Brunese L. Errors in neuroradiology. Radiol Med 2015; 120: 795-801.
14. Muccio CF, Di Blasi A, Esposito G, Brunese L, D'Arco F, Caranci F. Perfusion and spectroscopy magnetic resonance imaging in a case of lymphocytic vasculitis mimicking brain tumor. Pol J Radiol 2013; 78: 66-69.
15. Briganti F, Delehaye L, Leone G, Sicignano C, Buono G, Marseglia M, Caranci F, Tortora F, Maiuri F. Flow diverter device for the treatment of small middle cerebral artery aneurysms. J Neurointervent Surg 2016; 8: 287-294.
16. Frassica FJ, Waltrip RL, Sponseller PD, Ma LD, McCarthy EF, Jr. Clinicopathologic features and treatment of osteoid osteoma and osteoblastoma in children and adolescents. Orthop Clin North Am 1996; 27: 559-74.
17. O'Connell JX, Nanthakumar SS, Nielsen GP, Rosenberg AE. Osteoid osteoma: the uniquely innervated bone tumor. Mod Pathol 1998; 11: 175-80.
18. Graham GN, Browne H. Primary bony tumors of the pediatric spine. Yale J Biol Med 2001; 74: 1-8.
19. De Smet L. Synovitis of the wrist joint caused by an intraarticular perforation of an osteoid osteoma of the radial styloid. Clin Rheumatol 2000; 19: 229-30.
20. Lee EH, Shafi M, Hui JH. Osteoid osteoma: a current review. J Pediatr Orthop 2006; 26: 695-700.

21. Jordan RW, Koc T, Chapman AW, Taylor HP. Osteoid osteoma of the foot and ankle--A systematic review. Foot Ankle Surg 2015; 21: 228-34.
22. Muccio CF, Caranci F, D'Arco F, Cerase A, De Lipsis L, Esposito G, Tedeschi E, Andreula C. Magnetic resonance features of pyogenic brain abscesses and differential diagnosis using morphological and functional imaging studies: A pictorial essay. J Neuroradiol 2014; 41: 153-167.
23. Caranci F, Briganti F, La Porta M, Antinolfi G, Cesarano E, Fonio P, Brunese L, Coppolino F. Magnetic resonance imaging in brachial plexus injury. Musculoskeletal Surg 2013; 97: S181-S190.
24. Caranci F, Napoli M, Cirillo M, Briganti G, Brunese L, Briganti F. Basilar artery hypoplasia. Neuroradiol J 2012; 25: 739-743. 25. Di Zazzo E, Porcile C, Bartollino S, Moncharmont B. Critical Function of PRDM2 in the Neoplastic Growth of Testicular Germ Cell Tumors Biology (Basel) 2016; 5:
26. Nurzynska D, DiMeglio F, Castaldo C, Latino F, Romano V, Miraglia R, Guerra G, Brunese L, Montagnani S. Flatfoot in children: Anatomy of decision making. Ital J Anat Embryol 2012; 117: 98-106.
27. Dragoni S, Turin I, Laforenza U, Potenza DM, Bottino C, Glasnov TN, Prestia M, Ferulli F, Saitta A, Mosca A, Guerra G, Rosti V, Luinetti O, Ganini C, Porta C, Pedrazzoli P, Tanzi F, Montagna D, Moccia F. Store-operated Ca2+ entry does not control proliferation in primary cultures of human metastatic renal cellular carcinoma. Biomed Res Int 2014; 2014: 739494.
28. Cappabianca S, Scuotto A, Iaselli F, Pignatelli di Spinazzola N, Urraro F, Sarti G, Montemarano M, Grassi R, Rotondo A. Computed tomography and magnetic resonance angiography in the evaluation of aberrant origin of the external carotid artery branches. Surg Radiol Anat 2012; 34: 393-9.
29. Barile A, Arrigoni F, Bruno F, Guglielmi G, Zappia M, Reginelli A, Ruscitti P, Cipriani P, Giacomelli R, Brunese L, Masciocchi C. Computed Tomography and MR Imaging in Rheumatoid Arthritis. Radiol Clin North Am 2017;
30. Mandato Y, Reginelli A, Galasso R, Iacobellis F, Berritto D, Cappabianca S. Errors in the radiological evaluation of the alimentary tract: part I. Semin Ultrasound CT MR 2012; 33: 300-7.
31. d'Apuzzo F, Cappabianca S, Ciavarella D, Monsurro A, Silvestrini-Biavati A, Perillo L. Biomarkers of periodontal tissue remodeling during orthodontic tooth movement in mice and men: overview and clinical relevance. Scientific World Journal 2013; 2013: 105873.
32. Briganti F, Tedeschi E, Leone G, Marseglia M, Cicala D, Giamundo M, Napoli M, Caranci F. Endovascular treatment of vertebro-vertebral arteriovenous fistula. A report of three cases and literature review. Neuroradiol J 2013; 26: 339-346.
33. Cappabianca S, Colella G, Russo A, Pezzullo M, Reginelli A, Iaselli F, Rotondo A. Maxillofacial fibrous dysplasia: personal experience with gadoliniumenhanced magnetic resonance imaging. Radiol Med 2008; 113: 1198-210.
34. Cappabianca S, Colella G, Pezzullo MG, Russo A, Iaselli F, Brunese L, Rotondo A. Lipomatous lesions of the head and neck region: Imaging findings in comparison with histological type. Radiol Med 2008; 113: 758-770.
35. Splendiani A, Ferrari F, Barile A, Masciocchi C, Gallucci M. Occult neural foraminal stenosis caused by association between disc degeneration and facet joint osteoarthritis: Demonstration with dedicated upright MRI system. Radiol Med 2014; 119: 164-174.
36. Hashemi J, Gharahdaghi M, Ansaripour E, Jedi F, Hashemi S. Radiological features of osteoid osteoma: pictorial review. Iran J Radiol 2011; 8: 182-9.
37. Lanza E, Thouvenin Y, Viala P, Sconfienza LM, Poretti D, Cornalba G, Sardanelli F, Cyteval C. Osteoid osteoma treated by percutaneous thermal ablation: when do we fail? A systematic review and guidelines for future reporting. Cardiovasc Intervent Radiol 2014; 37: 1530-9.
38. Mainini AP, Monaco C, Pescatori LC, De Angelis C, Sardanelli F, Sconfienza LM, Mauri G. Image-guided thermal ablation of benign thyroid nodules. J Ultrasound 2017; 20: 11-22.
39. Mauri G, Sconfienza LM, Pescatori LC, Fedeli MP, Ali M, Di Leo G, Sardanelli F. Technical success, technique efficacy and complications of minimally-invasive imaging-guided percutaneous ablation procedures of breast cancer: A systematic review and meta-analysis. Eur Radiol 2017; 27: 3199-3210.
40. Mauri G, Sconfienza LM. Image-guided thermal ablation might be a way to compensate for image deriving cancer overdiagnosis. Int J Hyperthermia 2016; 1-2.
41. Mauri G, Sconfienza LM. Percutaneous ablation holds the potential to substitute for surgery as first choice treatment for symptomatic benign thyroid nodules. Int J Hyperthermia 2016; 1-2.
42. Mauri G, Cova L, Monaco CG, Sconfienza LM, Corbetta S, Benedini S, Ambrogi F, Milani V, Baroli A, Ierace T, Solbiati L. Benign thyroid nodules treatment using percutaneous laser ablation (PLA) and radiofrequency ablation (RFA). Int J Hyperthermia 2016; 1-5.
43. Mauri G, Orsi F, Sconfienza LM. Systemic Effects of Local Tumor Ablation: Oncogenesis and Antitumor Induced Immunity. Radiology 2016; 279: 322-3.
44. Pescatori LC, Sconfienza LM, Mauri G. The role of contrast-enhanced ultrasonography in image-guided liver ablations. Ultrasonography 2016; 35: 87-8.
45. Gallucci M, Limbucci N, Paonessa A, Splendiani A. Degenerative disease of the spine. Neuroimaging Clin N Am 2007; 17: 87-103.
46. Ghanem I. The management of osteoid osteoma: updates and controversies. Curr Opin Pediatr 2006; 18: 36-41.
47. Barile A, La Marra A, Arrigoni F, Mariani S, Zugaro L, Splendiani A, Di Cesare E, Reginelli A, Zappia M, Brunese L, Duka E, Carrafiello G, Masciocchi C. Anaesthetics, steroids and platelet-rich plasma (PRP) in ultrasound-guided musculoskeletal procedures. Br J Radiol 2016; 89:
48. Zappia M, Carfora M, Romano AM, Reginelli A, Brunese

L, Rotondo A, Castagna A. Sonography of chondral print on humeral head. Skelet. Radiol. 2016; 45: 35-40.
49. Zappia M, Di Pietto F, Aliprandi A, Pozza S, De Petro P, Muda A, Sconfienza LM. Multi-modal imaging of adhesive capsulitis of the shoulder. Insights Imaging 2016; 7: 365-71.
50. Russo A, Reginelli A, Zappia M, Rossi C, Fabozzi G, Cerrato M, Macarini L, Coppolino F. Ankle fracture: radiographic approach according to the Lauge-Hansen classification. Musculoskelet Surg 2013; 97 Suppl 2: S155-60.
51. Russo A, Zappia M, Reginelli A, Carfora M, D'Agosto GF, La Porta M, Genovese EA, Fonio P. Ankle impingement: a review of multimodality imaging approach. Musculoskelet Surg 2013; 97 Suppl 2: S161-8.
52. Zappia M, Cuomo G, Martino MT, Reginelli A, Brunese L. The effect of foot position on Power Doppler Ultrasound grading of Achilles enthesitis. Rheumatol Int 2016; 36: 871-874.
53. Reginelli A, Zappia M, Barile A, Brunese L. Strategies of imaging after orthopedic surgery. Musculoskeletal Surg 2017; 101:
54. Pinto A, Brunese L, Pinto F, Reali R, Daniele S, Romano L. The Concept of Error and Malpractice in Radiology. Semin Ultrasound CT MRI 2012; 33: 275-279.
55. Zappia M, Reginelli A, Russo A, D'Agosto GF, Di Pietto F, Genovese EA, Coppolino F, Brunese L. Long head of the biceps tendon and rotator interval. Musculoskeletal Surg 2013; 97: S99-S108.
56. Pinto A, Brunese L, Daniele S, Faggian A, Guarnieri G, Muto M, Romano L. Role of Computed Tomography in the Assessment of Intraorbital Foreign Bodies. Semin. Ultrasound CT MRI 2012; 33: 392-395.
57. Pinto A, Brunese L, Pinto F, Acampora C, Romano L. E-learning and education in radiology. Eur J Radiol 2011; 78: 368-371.
58. Pinto A, Reginelli A, Pinto F, Sica G, Scaglione M, Berger FH, Romano L, Brunese L. Radiological and practical aspects of body packing. Br J Radiol 2014; 87:
59. Iaccarino C, Tedeschi E, Rapanà A, Massarelli I, Belfiore G, Quarantelli M, Bellotti A. Is the distance between mammillary bodies predictive of a thickened third ventricle floor? J Neurosurg 2009; 110: 852-857.
60. Muto M, Perrotta V, Guarnieri G, Lavanga A, Vassallo P, Reginelli R, Rotondo A. Vertebroplasty and kyphoplasty: Friends or foes? Radiol Med 2008; 113: 1171-1184.
61. Reginelli A, Pinto A, Russo A, Fontanella G, Rossi C, Del Prete A, Zappia M, D'Andrea A, Guglielmi G, Brunese L. Sharp penetrating wounds: spectrum of imaging findings and legal aspects in the emergency setting. Radiol Med 2015; 120: 856-865.
62. Liu PT, Kujak JL, Roberts CC, de Chadarevian JP. The vascular groove sign: a new CT finding associated with osteoid osteomas. AJR Am J Roentgenol 2011; 196: 168-73.
63. Di Cesare E, Gennarelli A, Di Sibio A, Felli V, Perri M, Splendiani A, Gravina GL, Barile A, Masciocchi C. 320-row coronary computed tomography angiography (CCTA) with automatic exposure control (AEC): effect of 100 kV versus 120 kV on image quality and dose exposure. Radiol Med 2016; 121: 618-625.
64. Regine G, Stasolla A, Miele V. Multidetector computed tomography of the renal arteries in vascular emergencies. Eur J Radiol 2007; 64: 83-91.
65. De Cecco CN, Buffa V, Fedeli S, Vallone A, Ruopoli R, Luzietti M, Miele V, Rengo M, Maurizi Enrici M, Fina P, Laghi A, David V. Preliminary experience with abdominal dual-energy CT (DECT): True versus virtual nonenhanced images of the liver. Radiol Med 2010; 115: 1258-1266.
66. Miele V, Di Giampietro I. Diagnostic imaging in emergency. Salute Soc 2014; 127-141.
67. Miele V, Di Giampietro I, Ianniello S, Pinto F, Trinci M. Diagnostic imaging in pediatric polytrauma management. Radiol Med 2014; 120: 33-49.
68. Barile A, Bruno F, Mariani S, Arrigoni F, Reginelli A, De Filippo M, Zappia M, Splendiani A, Di Cesare E, Masciocchi C. What can be seen after rotator cuff repair: a brief review of diagnostic imaging findings. Musculoskeletal Surg 2017; 101: 3-14.
69. Zappia M, Aliprandi A, Pozza S, Doniselli FM, Gitto S, Sconfienza LM. How is shoulder ultrasound done in Italy? A survey of clinical practice. Skeletal Radiol 2016; 45: 1629-1634.
70. Perrotta FM, Astorri D, Zappia M, Reginelli A, Brunese L, Lubrano E. An ultrasonographic study of enthesis in early psoriatic arthritis patients naive to traditional and biologic DMARDs treatment. Rheumatol Int 2016; 36: 1579-1583.
71. De Filippo M, Corsi A, Evaristi L, Bertoldi C, Sverzellati N, Averna R, Crotti P, Bini G, Tamburrini O, Zompatori M, Rossi C. Critical issues in radiology requests and reports. Radiol Med 2011; 116: 152-62.
72. Ingegnoli A, Corsi A, Verardo E, De Filippo M, Sverzellati N, Zompatori M. Uncommon causes of tracheobronchial stenosis and wall thickening: MDCT imaging. Radiol Med 2007; 112: 1132-41.
73. Zoccali C, Arrigoni F, Mariani S, Bruno F, Barile A, Masciocchi C. An unusual localization of chondroblastoma: The triradiate cartilage; from a case report a reconstructive technique proposal with imaging evolution. J Clin Orthop Trauma 2017; 8: S48-S52.
74. Arrigoni F, Barile A, Zugaro L, Fascetti E, Zappia M, Brunese L, Masciocchi C. CT-guided radiofrequency ablation of spinal osteoblastoma: treatment and long-term follow-up. Int J Hyperthermia 2017; 1-7.
75. Barile A, Arrigoni F, Zugaro L, Zappia M, Cazzato RL, Garnon J, Ramamurthy N, Brunese L, Gangi A, Masciocchi C. Minimally invasive treatments of painful bone lesions: state of the art. Med Oncol 2017; 34:
76. Davies M, Cassar-Pullicino VN, Davies AM, McCall IW, Tyrrell PN. The diagnostic accuracy of MR imaging in osteoid osteoma. Skeletal Radiol 2002; 31: 559-69.
77. Masciocchi C, Arrigoni F, Ferrari F, Giordano AV, Iafrate S, Capretti I, Cannizzaro E, Reginelli A, Ierardi AM, Floridi C, Angileri AS, Brunese L, Barile A. Uterine fibroid thera-

py using interventional radiology mini-invasive treatments: current perspective. Med. Oncol. 2017; 34:
78. Arrigoni F, Barile A, Zugaro L, Splendiani A, Di Cesare E, Caranci F, Ierardi AM, Floridi C, Angileri AS, Reginelli A, Brunese L, Masciocchi C. Intra-articular benign bone lesions treated with Magnetic Resonance-guided Focused Ultrasound (MRgFUS): imaging follow-up and clinical results. Med Oncol 2017; 34:
79. Di Pietto F, Chianca V, de Ritis R, Cesarano E, Reginelli A, Barile A, Zappia M, Ginolfi L. Postoperative imaging in arthroscopic hip surgery. Musculoskeletal Surg 2017; 101: 43-49.
80. Splendiani A, D'Orazio F, Patriarca L, Arrigoni F, Caranci F, Fonio P, Brunese L, Barile A, Di Cesare E, Masciocchi C. Imaging of post-operative spine in intervertebral disc pathology. Musculoskeletal Surg 2017; 101: 75-84.
81. De Filippo M, Pesce A, Barile A, Borgia D, Zappia M, Romano A, Pogliacomi F, Verdano M, Pellegrini A, Johnson K. Imaging of postoperative shoulder instability. Musculoskeletal Surg 2017; 101: 15-22.
82. Minoia C, Maggialetti N, Ferrari C, Brunese L, Rubini G, Guarini A. Can diffusion-weighed whole-body magnetic resonance imaging with body signal suppression play a role in the management of lymphoma patients? J B.U.ON. 2016; 21: 282-283.
83. Brunese L, Greco B, Setola FR, Lassandro F, Guarracino MR, De Rimini M, Piccolo S, De Rosa N, Muto R, Bianco A, Muto P, Grassi R, Rotondo A. Non-small cell lung cancer evaluated with quantitative contrast-enhanced CT and PET-CT: Net enhancement and standardized uptake values are related to tumour size and histology. Med Sci Monit 2013; 19: 95-101.
84. Cappabianca S, Porto A, Petrillo M, Greco B, Reginelli A, Ronza F, Setola F, Rossi G, Di Matteo A, Muto R, De Rimini ML, Piccolo S, Catalano M, Muto P, De Rosa N, Barra E, De Rosa I, Antinolfi F, Antinolfi G, Caputi M, Brunese L, Grassi R, Rotondo A. Preliminary study on the correlation between grading and histology of solitary pulmonary nodules and contrast enhancement and [18F] fluorodeoxyglucose standardised uptake value after evaluation by dynamic multiphase CT and PET/CT. J Clin Pathol 2011; 64: 114-119.
85. Maggialetti N, Ferrari C, Minoia C, Asabella AN, Ficco M, Loseto G, De Tullio G, de Fazio V, Calabrese A, Guarini A, Rubini G, Brunese L. Role of WB-MR/DWIBS compared to 18F-FDG PET/CT in the therapy response assessment of lymphoma. Radiol Med 2016; 121: 132-143.
86. Pinto A, Pinto F, Faggian A, Rubini G, Caranci F, Macarini L, Genovese EA, Brunese L. Sources of error in emergency ultrasonography. Crit Ultrasound J 2013; 5: 1-5.
87. Kneisl JS, Simon MA. Medical management compared with operative treatment for osteoid-osteoma. J Bone Joint Surg Am 1992; 74: 179-85.
88. Cazzato RL, Garnon J, Ramamurthy N, Koch G, Tsoumakidou G, Caudrelier J, Arrigoni F, Zugaro L, Barile A, Masciocchi C, Gangi A. Percutaneous image-guided cryoablation: current applications and results in the oncologic field. Med Oncol 2016; 33:
89. Masciocchi C, Zugaro L, Arrigoni F, Gravina GL, Mariani S, La Marra A, Zoccali C, Flamini S, Barile A. Radiofrequency ablation versus magnetic resonance guided focused ultrasound surgery for minimally invasive treatment of osteoid osteoma: a propensity score matching study. Eur Radiol 2016; 26: 2472-2481.
90. Ferrari F, Arrigoni F, Miccoli A, Mascaretti S, Fascetti E, Mascaretti G, Barile A, Masciocchi C. Effectiveness of Magnetic Resonance-guided Focused Ultrasound Surgery (MRgFUS) in the uterine adenomyosis treatment: technical approach and MRI evaluation. Radiol Med 2016; 121: 153-161.
91. Rosenthal DI, Hornicek FJ, Wolfe MW, Jennings LC, Gebhardt MC, Mankin HJ. Percutaneous radiofrequency coagulation of osteoid osteoma compared with operative treatment. J Bone Joint Surg Am 1998; 80: 815-21.
92. Cantwell CP, Obyrne J, Eustace S. Current trends in treatment of osteoid osteoma with an emphasis on radiofrequency ablation. Eur Radiol 2004; 14: 607-17.
93. Karagoz E, Ozel D, Ozkan F, Ozel BD, Ozer O, Coskun ZU. Effectiveness of Computed Tomography Guided Percutaneous Radiofrequency Ablation Therapy for Osteoid Osteoma: Initial Results and Review of the Literature. Pol J Radiol 2016; 81: 295-300.
94. Masciocchi C, Arrigoni F, Marra AL, Mariani S, Zugaro L, Barile A. Treatment of focal benign lesions of the bone: MRgFUS and RFA. Br J Radiol 2016; 89:
95. Ierardi AM, Xhepa G, Piffaretti G, Bacuzzi A, Tozzi M, Carbone M, Barile A, Squillaci E, Fonio P, Brunese L, Carrafiello G. Clinical experience with Angiojet: A comprehensive review. Int Angiol 2015; 34: 1-14.
96. Albisinni U, Facchini G, Spinnato P, Gasbarrini A, Bazzocchi A. Spinal osteoid osteoma: efficacy and safety of radiofrequency ablation. Skeletal Radiol 2017; 46: 1087-1094.
97. Miyazaki M, Arai Y, Myoui A, Gobara H, Sone M, Rosenthal DI, Tsushima Y, Kanazawa S, Ehara S, Endo K. Phase I/II Multi-Institutional Study of Percutaneous Radiofrequency Ablation for Painful Osteoid Osteoma (JIVROSG-0704). Cardiovasc Intervent Radiol 2016; 39: 1464-70.
98. Wang B, Han SB, Jiang L, Yuan HS, Liu C, Zhu B, Liu ZJ, Liu XG. Percutaneous radiofrequency ablation for spinal osteoid osteoma and osteoblastoma. Eur Spine J 2017; 26: 1884-1892.
99. Cakar M, Esenyel CZ, Seyran M, Tekin AC, Adas M, Bayraktar MK, Coskun U. Osteoid osteoma treated with radiofrequency ablation. Adv Orthop 2015; 2015: 807274.
100. Lassalle L, Campagna R, Corcos G, Babinet A, Larousserie F, Stephanazzi J, Feydy A. Therapeutic outcome of CT-guided radiofrequency ablation in patients with osteoid osteoma. Skeletal Radiol 2017; 46: 949-956.
101. Motamedi D, Learch TJ, Ishimitsu DN, Motamedi K, Katz MD, Brien EW, Menendez L. Thermal ablation of

osteoid osteoma: overview and step-by-step guide. Radiographics 2009; 29: 2127-41.
102. Zoccali C, Rossi B, Zoccali G, Barbarino E, Gregori L, Barile A, Masciocchi C. A new technique for biopsy of soft tissue neoplasms: A preliminary experience using MRI to evaluate bleeding. Minerva Med 2015; 106: 117-120.
103. Arrigoni F, Gregori LM, Zugaro L, Barile A, Masciocchi C. MRgFUS in the treatment of MSK lesions: A review based on the experience of the university of L'aquila, Italy. Transl Cancer Res 2014; 3: 442-448.
104. Masciocchi C, Conchiglia A, Gregori LM, Arrigoni F, Zugaro L, Barile A. Critical role of HIFU in musculoskeletal interventions. Radiol Med 2014; 119: 470-475.
105. Masciocchi C, Conti L, D'Orazio F, Conchiglia A, Lanni G, Barile A, Errors in musculoskeletal MRI, Errors in Radiology, Springer-Verlag Milan 2012, pp. 209-217.
106. Barile A, Regis G, Masi R, Maggiori M, Gallo A, Faletti C, Masciocchi C. Musculoskeletal tumours: Preliminary experience with perfusion MRI. Radiol Med 2007; 112: 550-561.
107. Arikan Y, Yavuz U, Lapcin O, Sokucu S, Ozkan B, Kabukcuoglu Y. Percutaneous radiofrequency ablation for osteoid osteoma under guidance of threedimensional fluoroscopy. J Orthop Surg (Hong Kong) 2016; 24: 398-402.
108. Barile A, Limbucci N, Splendiani A, Gallucci M, Masciocchi C. Spinal injury in sport. Eur J Radiol 2007; 62: 68-78.
109. Dialetto G, Reginelli A, Cerrato M, Rossi G, Covino FE, Manduca S, Lassandro F. Endovascular stent-graft treatment of thoracic aortic syndromes: a 7-year experience. Eur J Radiol 2007; 64: 65-72.
110. Belfiore G, Belfiore MP, Reginelli A, Capasso R, Romano F, Ianniello GP, Cappabianca S, Brunese L. Concurrent chemotherapy alone versus irreversible electroporation followed by chemotherapy on survival in patients with locally advanced pancreatic cancer. Med Oncol 2017; 34:
111. Reginelli A, Silvestro G, Fontanella G, Sangiovanni A, Conte M, Nuzzo I, Calvanese M, Traettino M, Ferraioli P, Grassi R, Manzo R, Cappabianca S. Validation of DWI in assessment of radiotreated bone metastases in elderly patients. Int J Surg 2016; 33 Suppl 1: S148-53.
112. Floridi C, Reginelli A, Capasso R, Fumarola E, Pesapane F, Barile A, Zappia M, Caranci F, Brunese L. Percutaneous needle biopsy of mediastinal masses under C-arm conebeam CT guidance: diagnostic performance and safety. Med Oncol 2017; 34: 67.
113. Reginelli A, Vanzulli A, Sgrazzutti C, Caschera L, Serra N, Raucci A, Urraro F, Cappabianca S. Vascular microinvasion from hepatocellular carcinoma: CT findings and pathologic correlation for the best therapeutic strategies. Med Oncol 2017; 34: 93.
114. Schnapauff D, Streitparth F, Johrens K, Wieners G, Collettini F, Hamm B, Gebauer B. CT-guided radiofrequency ablation of osteoid osteoma using a novel battery-powered drill. Skeletal Radiol 2015; 44: 695-701.
115. Vanderschueren GM, Taminiau AH, Obermann WR, Bloem JL. Osteoid osteoma: clinical results with thermocoagulation. Radiology 2002; 224: 82-6.
116. Spennato P, Rapanà A, Sannino E, Iaccarino C, Tedeschi E, Massarelli I, Bellotti A, Schonauer M. Retropharyngeal cerebrospinal fluid collection as a cause of postoperative dysphagia after anterior cervical discectomy. Surg Neurol 2007 67:499-503.
117. Brunese L, Romeo A, Iorio S, Napolitano G, Fucili S, Zeppa P, Vallone G, Lombardi G, Bellastella A, Biondi B, Sodano A. Thyroid B-flow twinkling sign: A new feature of papillary cancer. Eur J Endocrinol 2008; 159: 447-451.

Received: 15 September 2017
Accepted: 20 December 2017
Correspondence:
Umberto Russo
Department of Radiology, Parma Hospital,
Via Gramsci 14 - 43126 Parma, Italy
E-mail: umberto.russo1@studenti.unipr.it